Coordination Chemistry Reviews 254 (2010) 2492–2504

Contents lists available at ScienceDirect

Coordination Chemistry Reviews

journal homepage: www.elsevier.com/locate/ccr

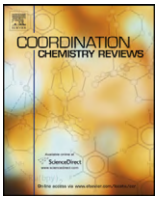

Review

Catalytic hydrogen production at cobalt centres

Sebastian Losse[a,b], Johannes G. Vos[c], Sven Rau[b,*]

[a] *Institut für Anorganische und Analytische Chemie, Friedrich-Schiller-Universität Jena, August-Bebel-Str. 2, 07743 Jena, Germany*
[b] *Lehrstuhl für Anorganische und Allgemeine Chemie, Friedrich-Alexander-Universität Erlangen-Nürnberg, Egerlandstr. 1, 91058 Erlangen, Germany*
[c] *Solar Energy Conversion SRC, School of Chemical Sciences, Dublin City University, Dublin 9, Ireland*

Contents

ARTICLE INFO

Article history:
Received 13 January 2010
Accepted 15 June 2010
Available online 23 June 2010

Keywords:
Photocatalysis
Ruthenium
Cobalt
Hydrogen

ABSTRACT

The catalytic properties of a wide range of cobalt complexes with respect to proton reduction are discussed. Electrocatalytic as well as photocatalytic systems are addressed and to allow comparison between the different systems reported considerable attention is paid to the reaction conditions used. For the photocatalytic proton reduction a range of ruthenium, iridium and rhenium complexes are discussed as potential photosensitizers. The photocatalytic systems are discussed in detail and issues such as the nature of the sacrificial agent and the solvents used. Both intermolecular and intramolecular photocatalysis are considered. The results obtained are considered with respect to the need to the development of sustainable energy sources.

1. Introduction

The development of carbon neutral energy sources is of fundamental importance for the future growth of our civilization. One of the most promising approaches towards this aim is the conversion of solar energy into storable fuels like hydrogen or via reduction of carbon dioxide [1,2]. Within this area two general options may be considered. Firstly to capture sunlight using conventional solar cells and perform the initial charge separation generating an electrical potential which than can be used to drive electrocatalytical processes [3]. The other concept uses the known ability of certain dyes to generate high energy electrons upon excitation with light. These electrons may be used to perform redox reactions provided the other partners in this reaction possess the appropriate redox properties. Cobalt complexes have been investigated in detail as catalysts for both hydrogen evolution and CO_2 reduction in both approaches during the past three decades. The process of water splitting can be divided into two reactions: (i) water oxidation, to yield O_2 and (ii) water reduction, producing H_2. Catalysts for oxidizing water are rare but known [3–6]. In this review we will focus on water reduction using electrical potentials or light for the hydrogen evolution at cobalt catalysts. We discuss the catalytic

---

* Corresponding author. Tel.: +49 9131 8527396; fax: +49 9131 8527367.
E-mail address: sven.rau@chemie.uni-erlangen.de (S. Rau).

0010-8545/$ – see front matter
doi:10.1016/j.ccr.2010.06.004

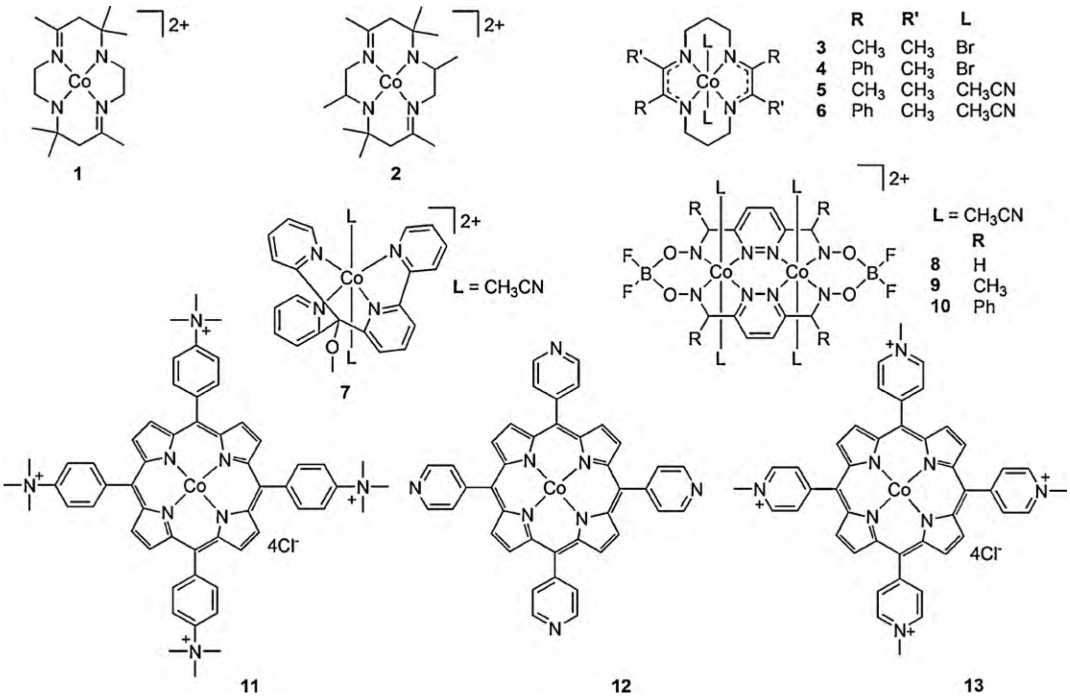

Fig. 1. Macrocyclic cobalt complexes for electrocatalytic hydrogen production.

properties of cobalt complexes towards hydrogen production and consider potential future applications. Electrocatalytic reactions are discussed because of their analogy to photocatalytic processes.

2. Electrocatalysis

2.1. Cobalt macrocycles and porphyrins

The application of macrocyclic cobalt complexes as catalysts in electrochemical reduction of CO_2 has been investigated by Eisenberg et al. Tetraazamacrocyclic compounds **1** and **2** catalyse CO and H_2 formation in water containing acetonitrile solution at potentials of −1.6 V (**1**) and −1.5 V (**2**) *vs.* SCE, only slightly less negative than observed for direct electrolysis which requires potentials more negative than −2 V *vs.* SCE [7]. An interesting observation is that these complexes evolve CO and H_2 only in the presence of CO_2, no CO or H_2 was detected when the cobalt complexes were electrolyzed under Ar or N_2. When the same reaction with **2** was performed in CH_3CN/H_2O under N_2 only H_2 was formed. Because of the need of a proton source like water to evolve hydrogen a cobalt hydride intermediate has been postulated.

Cobalt complexes **3** and **5** show quantitative Faradaic yields by bulk electrolysis at −0.58 V *vs.* SCE in a CH_3CN solution containing $TsOH{\cdot}H_2O$ or $HBF_4{\cdot}Et_2O$ as an acid, which acts as the proton source. Turnover values > 5 were achieved. With **4** and **6** the Faradaic yield at −0.48 V *vs.* SCE is 20–25%, less than observed for **3** and **5**. This is ascribed to the observed deactivation of the catalyst after two turnovers.

Tetradentate polypyridine cobalt complexes like **7** are also known electrocatalysts for proton reduction which are able to operate media containing up to 50% of water (1:1 water:acetonitrile). With an applied potential of −1.0 V *vs.* SCE (carbon electrode) a TOF of 40 was measured using TFA as the proton source [8]. Peters et al. described dicobalt macrocycles **8**–**10** showing catalytic waves by addition of 2,6-dichloroanilinium tetrafluoroborate at around −0.3 V *vs.* SCE for **8** and −0.7 V *vs.* SCE for **9** whereas **9** shows a higher current by adding acid with respect to **8**. EPR spectroscopic investigations of an electrochemically formed mixed valent Co(II)–Co(I) complex suggest the presence of a low spin Co(II) centre in tetragonally distorted coordination environment [9].

Cobalt porphyrins can be used as electrocatalysts in the hydrogen production reaction from water. For example the water soluble cobalt complexes of porphyrins *meso*-tetrakis(N,N,N-trimethylanilinium-4-yl)porphyrin chloride (CoTMAP, **11**), *meso*-tetrapyrid-4-ylporphyrin (CoTPyP, **12**) and *meso*-tetrakis(N-methylpyridinium-4-yl)porphyrin chloride (CoTMPyP, **13**) are good catalysts for the reduction of water to hydrogen at a potential of −0.95 V *vs.* SCE at a Hg-pool electrode in 0.1 M trifluoroacetic

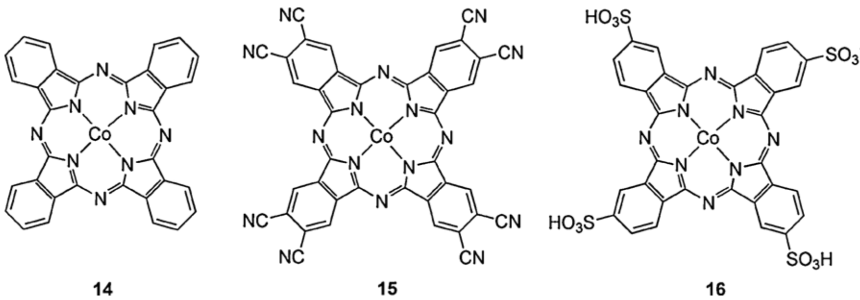

Fig. 2. Cobalt phthalocyanine complexes able to catalyse proton reduction.

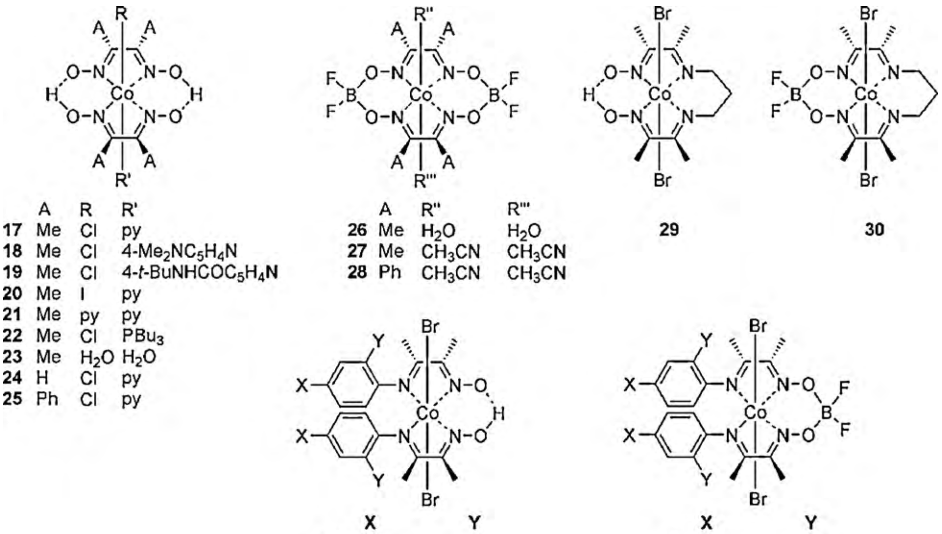

	A	R	R'
17	Me	Cl	py
18	Me	Cl	4-$Me_2NC_5H_4N$
19	Me	Cl	4-*t*-$BuNHCOC_5H_4N$
20	Me	I	py
21	Me	py	py
22	Me	Cl	PBu_3
23	Me	H_2O	H_2O
24	H	Cl	py
25	Ph	Cl	py

	A	R''	R'''
26	Me	H_2O	H_2O
27	Me	CH_3CN	CH_3CN
28	Ph	CH_3CN	CH_3CN

29 **30**

	X	Y
31	H	H
32	OMe	H
33	CH_2COOH	H
34	H	Ph

	X	Y
35	H	H
36	OMe	H
37	CH_2COOH	H
38	H	Ph

Fig. 3. Different types of glyoxime cobalt complexes.

acid with a current efficiency > 90% [10,11]. The complexes show little decomposition but show a tendency for electrode adsorption. With decreasing pH an increased H_2 production rate was observed. If **11** is incorporated into a Nafion film on a glassy carbon electrode a TON of 26 after 90 min at −0.95 V *vs.* SCE is achieved. However, mass charge transport efficiencies in these systems clearly limit the overall activity. Two H_2 evolution pathways have been considered. The first involves proton attack on a cobalt(III) hydride species (Eq. (1)) and a following reduction of Co(III) at an electrode or by Co(I). The second pathway involves a disproportionation reaction of the cobalt hydride (Eq. (2)). The potential for H_2 evolution is for all porphyrin based catalysts by about 0.6 V more positive than that of the cobalt macrocycles **1** and **2**.

$$\text{Co(III)–H}^- + \text{H}^+ \rightarrow \text{H}_2 + \text{Co(III)} \quad (1)$$

$$\text{Co(III)–H}^- \rightarrow \tfrac{1}{2}\text{H}_2 + \text{Co(II)} \quad (2)$$

Recent investigations of kinetics of the electron transfer reactions of cobalt glyoxime catalysts by Winkler and Gray et al. favour the homolytic process (Eq. (2)) as the main reaction pathway in hydrogen evolution at cobalt centres [12,13] (Fig. 1).

2.2. Cobalt phthalocyanines

The phthalocyanine cobalt complexes **14**–**16**, Fig. 2, acts as catalysts for electrochemical hydrogen production [14]. The compounds are incorporated in a poly(4-vinylpyridine-co-styrene) random copolymer film with a molar ratio of 4-vinylpyridine/styrene 9:1 coated on a graphite electrode. With the applied potential of −0.90 V *vs.* Ag/AgCl at pH 1.0, 0.1 mol L^{-1} aqueous phosphate buffer a turnover frequency (TOF) of $2 \times 10^5\ h^{-1}$ is obtained for **14**. The catalytic efficiency increases in the order **14** > **15** > **16**. Due to the incorporation of the catalyst in the polymer film charge transport through this matrix plays a significant role. Electron transfer can occur via physical diffusion and/or electron hopping. In the case of strong physical interaction or chemical bonding of the phthalocyanines physical diffusion can be neglected compared to the electron hopping mechanism. Otherwise physical diffusion is the dominant mechanism. Because of high turnover frequencies and the increased stability this method of using polymer modified electrodes with incorporated cobalt complexes has considerable potential for future applications.

2.3. Cobalt glyoximes

This class of compounds has received continuous attention not only due to the relative ease of preparation but also to their good axial ligand exchange properties. A variety of structurally related compounds possessing all the cobalt glyoxime motifs have been investigated (Fig. 3).

Compounds **17**–**26** were studied by Artero et al. using a weak acid, Et_3NH^+ ($pK_a = 10.75$) as the proton source in DMF or 1,2-dichloroethane on carbon electrodes [15]. With an applied potential of −0.90 V *vs.* Ag/AgCl (−0.945 V *vs.* SCE) in 1,2-dichloroethane, 0.2 mol L^{-1} Et_3NHCl a TON of 100 in 2.5 h was achieved for the hydrogen evolution reaction with **17** and no degradation was observed. The electrocatalytic activity depends on the amount of acid, Et_3NH^+. By adding 1.5, 3.0 and 10 equiv. of acid to the solution an irreversible cathodic wave appears

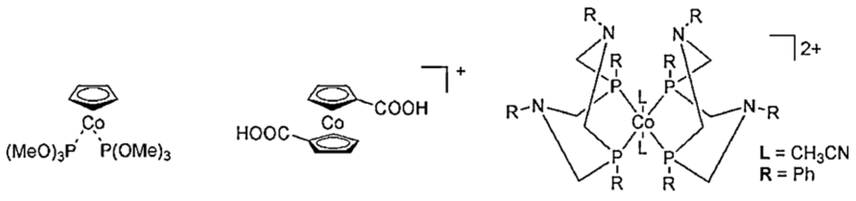

39 **40** **41**

Fig. 4. Cobalt cyclopentadienyl, phosphite and phosphine complexes for electrochemical hydrogen production.

Table 1

Comparison of reported potentials for electrochemical hydrogen evolution.

Comp. no.	Electrode	Potential (V) *vs.* SCE	Proton source	Solvent system	Product	TON	Ref.
1	Hg	–1.6[e]	H_2O	0.1 M KNO_3 in H_2O/CH_3CN 2:1(v/v) or H_2O only (CO_2)	CO + H_2	7.8/h (TOF)	[7]
2	Hg	–1.5[e]	H_2O	0.1 M KNO_3 in H_2O/CH_3CN 2:1(v/v) or H_2O only (CO_2)	CO + H_2	9/h (TOF)	[7]
3, **5**	Glassy carbon	–0.58[e]	$TsOH·H_2O/HBF_4·Et_2O$	CH_3CN, $TsOH·H_2O$ or $HBF_4·Et_2O$	H_2	>5	[17]
4, **6**	Glassy carbon	–0.48[e]	$TsOH·H_2O/HBF_4·Et_2O$	CH_3CN, $TsOH·H_2O$ or $HBF_4·Et_2O$	H_2	~2	[17]
7	Carbon	–1.0	TFA/H_2O	CH_3CN, H_2O, TFA	H_2	40/h (TOF)	[8]
11, **12**, **13**	Hg-pool	–0.95[e]	CF_3COOH, H_2O	0.1 M CF_3COOH	H_2	0.65 (20 min)	[10]
11	Glassy carbon/Nafion[a] film	–0.95	CF_3COOH	0.1 M CF_3COOH	H_2	26 (90 min)	[11]
14	P(VP-St)[b]/graphite	–0.95[c,e]	H_3PO_4, H_2O	pH 1.0, 0.1 mol L^{-1} aqueous phosphate buffer	H_2	2×10^5/h (TOF)	[14]
15	P(VP-St)[b]/graphite	–0.95[c,e]	H_3PO_4, H_2O	pH 1.0, 0.1 mol L^{-1} aqueous phosphate buffer	H_2	5×10^4/h (TOF)	[14]
16	P(VP-St)[b]/graphite	–0.95[c,e]	H_3PO_4, H_2O	pH 1.0, 0.1 mol L^{-1} aqueous phosphate buffer	H_2	~1.2×10^3/h (TOF)	[14]
17	Graphite	–0.95[c,e]	Et_3NHCl	1,2-Dichloroethane, 0.2 mol L^{-1} Et_3NHCl	H_2	100 (2.5 h)	[15]
26	Graphite	–0.95[c,e]	Et_3NHCl	1,2-Dichloroethane, 0.2 mol L^{-1} Et_3NHCl	H_2	80 (17 h)	[15]
27	Glassy carbon	–0.72[e]	CF_3COOH	CH_3CN, 0.045 M CF_3COOH	H_2	20 (1 h)	[16]
26, **27**	Glassy carbon	–0.95[c,e]	Et_3NHBF_4	DMF, Et_3NHBF_4	H_2	4.7/h (max. 80)	[15]
27	Glassy carbon	–0.55	CF_3COOH	CH_3CN, CF_3COOH	H_2	>5	[16]
26, **27**	Glassy carbon	–0.39	p-Cyanoanilinium	CH_3CN, p-cyanoanilinium	H_2	[d]	[18]
26, **27**	Glassy carbon	–0.57	p-Cyanoanilinium	DMF, p-cyanoanilinium	H_2	[d]	[18]
26, **27**	Glassy carbon	–0.57	$HBF_4·Et_2O$	DMF, $HBF_4·Et_2O$	H_2	[d]	[18]
28	Glassy carbon	–0.28	$HCl·Et_2O$	CH_3CN, $HCl·Et_2O$	H_2	>5	[16]
29	Graphite	–0.47	p-Cyanoanilinium	CH_3CN, p-cyanoanilinium	H_2	40 (3 h)	[19]
30	Graphite	–0.51	p-Cyanoanilinium	CH_3CN, p-cyanoanilinium	H_2	20 (3 h)	[19]
27	Adsorbed on glassy carbon	–0.90	H_3PO_4/H_2O	Phosphate buffer at pH 2	H_2	5×10^5 (7 h)	[20]
27	Adsorbed on glassy carbon	–0.95	CH_3COOH/H_2O	Acetate buffer, pH < 4.5	H_2	5×10^6 (16 h)	[20]
39	Hg-pool	–1.15[e]	H_2O, H^+	Aqueous solution, buffered to pH 5	H_2	20 (18 h)	[21]
40	Hg-pool	–0.9[e]	H_2O, H^+	KCl, phosphate buffer pH 6.5	H_2	[d]	[22]
42	Hg-pool	–0.7[e]	H_2O, H^+	KCl, phosphate buffer pH 4	H_2	[d]	[22]
41	Glassy carbon	–0.69	p-Bromoanilinium	CH_3CN, p-bromoanilinium tetrafluoroborate	H_2	90/s (TOF)	[23]

[a] Nafion = sulfonated polyfluorocarbon.

[b] P(VP-ST) = poly(4-vinylpyridine-co-styrene).

[c] Calculated from published data *vs.* Ag/AgCl.

[d] Not given.

[e] Bulk electrolysis.

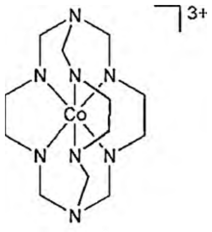

42

Fig. 5. Cobalt sepulchrate complex.

near the reversible Co(II)/Co(I) couple at −0.98 V *vs.* Ag/AgCl. By further increasing the acid concentration this wave shifts to a more negative potential while the Co(II)/Co(I) reversible wave disappears. The new catalytic wave was assigned to proton electroreduction. By changing the axial ligands or by introducing BF_2 groups the redox potentials of the complexes can be influenced. The potentials for the Co(II)/Co(I) couple, measured in DMF on a glassy carbon electrode *vs.* Ag/AgCl, 100 $mV\,s^{-1}$, following the order **26** (−0.55 V), **24** (−0.65 V), **25** (−0.70 V), **22** (−0.81 V), **19** (−0.97 V), **17**/**20**/**21**/**23** (−0.98 V) and **18** (−1.01 V). The activity for the hydrogen evolution reaction of compounds **22**, **24** and **25** is low on the cyclic voltammetry timescale. The redox properties of complexes **18** and **19** show no significant influence of the substituent compared to **17**, however a catalytic wave well separated from the Co(II)/Co(I) couple is observed. Electrolysis at a graphite electrode with 1.0 $mmol\,L^{-1}$ **26** at −0.90 V *vs.* Ag/AgCl, 0.2 $mol\,L^{-1}$ $Et_3NH(BF_4)$ in 1,2-dichloroethane produced H_2 with a TON of 80 within 17 h. Complex **23** was the least active. Mechanistic investigations suggested that in this solvent combination a heterolytic pathway for the hydrogen evolution may be considered. These data show that compared to the introduction of BF_2 groups, which induce rigidity of the ligand environment the nature of the substituent plays a secondarily role with regard to the catalytic activity. Further investigations of **26**–**28** with stronger acids like CF_3COOH, HCl, $TsOH{\cdot}H_2O$, $HBF_4{\cdot}Et_2O$ and p-cyanoanilinium in CH_3CN or DMF showed H_2 evolution [16–18]. Comparable results for **26** in DMF/Et_3NHCl are reported and electrocatalytic activity at an applied potential 350 mV more negative than that for the Co(II)/Co(I) reduction potential has been shown [18]. As noted for **17** the acid concentration plays a significant role in the electrocatalytic process. Detailed mechanistic studies performed here indicate that the catalytic pathways taken by the system strongly depend on the acid strength of the utilised proton donor. This correlation is also observed in the case of **27** and **28**. Optimal results for **27** could be achieved in DMF with Et_3NHBF_4, −0.9 V *vs.* Ag/AgCl, 4.7 TON h^{-1}, with a maximum TON of 80 [15] and in CH_3CN with CF_3COOH at −0.72 V *vs.* SCE, 20 TON h^{-1}, with a maximum TON of 20 [16]. For **28** in acidic CH_3CN with HCl or $HBF_4{\cdot}Et_2O$ hydrogen evolution is reported at a potential of −0.28 V *vs.* SCE with a TON > 5 [17].

Further substitution at the glyoxime moiety was investigated by Artero et al. using N-propyl chains instead of O–B–O or O–H–O for bridging two glyoxime ligands on one side where the second bridge is formed by the known motifs of O–H–O (**29**) or O–B–O (**30**). Bromide acts as the axial ligand. The propyl bridged cobalt complexes achieved turnover numbers after 3 h of 40 for **29** and 20 for **30** using p-cyanoanilinium as the proton source in CH_3CN at a graphite electrode with applied potentials of −0.78 V *vs.* Fc/Fc^+ (−0.47 V *vs.* SCE) and −0.82 V *vs.* Fc/Fc^+ (−0.51 V *vs.* SCE), respectively [19]. Under identical reaction conditions **27** yielded a TON of 50 after 3 h and an applied potential of −0.80 V *vs.* Fc/Fc^+. However, the propyl bridge leads to a higher stability of the cobalt complexes, judging from UV–vis and NMR studies. A large variety of N-aryl substituted glyoxime cobalt complexes were described by Peters et al. (**31**–**38**) [20]. All of them are active catalysts for hydrogen evolution exhibiting catalytic waves at potentials from −0.48 V *vs.* SCE (**31**) and −0.75 V *vs.* SCE (**32**) in CH_3CN and tosic acid at a glassy carbon electrode. All other compounds fall within this range. Detailed investigations are reported for **37**, which was adsorbed on ITO surfaces with a surface coverage corresponding roughly to a monolayer. This modified electrode was used in electrocatalysis showing electrocatalytic hydrogen production by increasing current of the reversible redox couple at −0.46 V *vs.* SCE when tosic acid was present. After several hours leaching of the catalyst was observed. The authors also investigated the behavior of adsorbed complex **27** at a glassy carbon electrode. With an applied potential of −0.90 V *vs.* SCE at pH 2 a TON of 5×10^5 after 7 h was achieved in a phosphate buffered solution. In acetate buffered solution with a pH < 4.5 a TON of 5×10^6 after 16 h was calculated. The applied potential was −0.95 V *vs.* SCE which makes clear that the adsorbed complex **27** is a better electrocatalyst when adsorbed at a glassy carbon electrode in aqueous media than the complex in solution.

2.4. Cobalt cyclopentadienyl and phosphine complexes

Kölle et al. investigated a cyclopentadienyl cobalt phosphite complex $[CpCo\{P(OMe)_3\}_2]$ (**39**) towards its applicability for electrocatalytic hydrogen evolution. In an aqueous solution buffered to pH 5 electrolyzed at −1.15 V *vs.* SCE at a Hg-pool electrode a TON of 20 was achieved after 18 h [21]. Grätzel, co-workers reported a cobaltocene complex **40** able to catalyse hydrogen evolution in KCl, phosphate buffer at pH 6.5 at −0.9 V *vs.* SCE [22]. DuBois et al. described a cobalt complex with two diphosphine ligands (**41**) [23]. In acetonitrile solution the complex loses one cyclic phosphine ligand by adding triflic acid giving the active catalyst. This compound gives a TOF of 90 s^{-1} with a catalytic wave at −1.00 V *vs.* Fc/Fc^+ (−0.69 V *vs.* SCE) in acetonitrile/p-bromoanilinium tetrafluoroborate at a glassy carbon electrode. The TOF is somewhat lower compared to the corresponding Nickel(II)-complex (350 s^{-1}), while the overpotential of the cobalt complex is lowered by 65 mV compared to the nickel catalyst. A potential explanation for this behavior is an involvement of the amine functions within the ligand framework in the activation of protons (Figs. 4 and 5).

2.5. Cobalt cage complexes

Hydrogen evolution utilising cobalt cage complexes has been investigated by Mau, Sasse, Sargeson as well as Grätzel et al. Both groups studied the electrochemical behavior of $[Co(sepulchrate)]^{3+}$ (**42**) complexes and similar derivatives [22,24]. Grätzel reported the electrochemical hydrogen evolution reaction at −0.7 V *vs.* SCE in KCl, phthalate buffer at pH 4 but the amount of produced H_2 was lower compared to that observed for **40** (Table 1).

3. Photocatalytic hydrogen production with cobalt catalysts

3.1. Co complexes of bpy and phen

One of the first photochemical experiments investigating the generation of hydrogen was performed by Lehn et al. in the early 1980s. The authors investigated the catalytic performance under visible light irradiation of the combination of the photosensitizer $[Ru(bpy)_3]^{2+}$ (bpy = 2,2′-bipyridine) (**PS1**, Fig. 6) with an electron relay like $CoCl_2$ (**43**) in aqueous solution. The main aim was to investigate the reduction of CO_2 to CO and/or H_2 formation [25]. In a degassed solution of acetonitrile/water with tripropylamine as an electron donor (3:1:1; v:v:v), **43** in the presence of **PS1**,

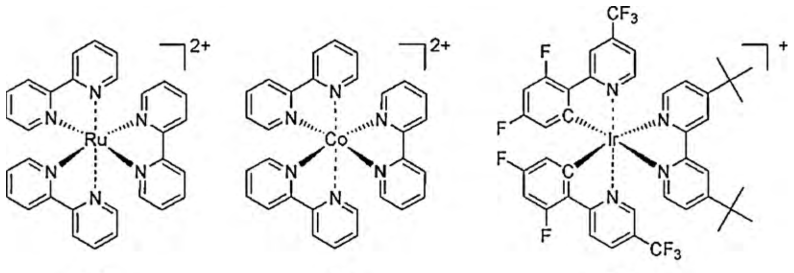

PS1 44 PS9

Fig. 6. Ruthenium and iridium photosensitizer and a cobalt bipyridine complex.

photochemically reduces CO_2 and water to CO and H_2 with a TON of 9 based on $CoCl_2$ after 22 h. When bpy is added to this solution of acetonitrile/water/triethylamine (up to 10 equiv. with respect to cobalt) to form $[Co(bpy)_3]^{2+}$ (**44**) *in situ* the amount of H_2 formed increases while CO production decreases. This observation emphases that occupation of the coordination sites of the cobalt centre hinders CO production and boosts H_2 formation. The generation of highly reducing Co(I) species able to reduce water and/or CO_2 was observed by irradiation of a solution of **43**, bpy, triethanolamine and **PS1** [26]. The nature of the reducing cobalt species without added bipyridine is unknown. The Co(I) key intermediate is most likely formed upon reduction of Co(II) by the photoreduced ruthenium photosensitizer **PS1**. The proposed mechanism proceeds via reductive quenching of **PS1** by a sacrificial electron donor and subsequent electron transfer to the Co(II)-species [27]. The so formed Co(I) species undergoes an oxidative addition of H^+ which results in the formation of a Co(III) hydride intermediate. Further protonation of the hydride results in the formation of H_2 (Eq. (1)). During these reactions a ligand exchange at the Co centre occurs, especially in the case of **44**, where one bpy is substituted by labile solvent molecules and/or protons. Interestingly, the hydrogen evolution reaction is nearly independent of temperature. Raising the temperature by about 10 °C has no influence on the hydrogen production rate. Protonation of the Co(III) hydride species at a rate which is outside the temperature defining reaction timescale has been put forward as explanation for this surprising finding. A similar system was also published by Sutin et al. where different ruthenium bipyridine and phenanthroline sensitizer complexes and **44** with triethanolamine or ascorbate as the electron donor produced H_2 [28,29]. Further investigations showed a high dependency of the catalytic activity on the nature of the electron donor, mostly tertiary amines, the organic solvent used, the photosensitizer and the cobalt ligand [27]. These observations seem relevant for most other photocatalytic processes known so far. Considering only the hydrogen evolution reaction the combination of **PS1** with **44** seems to be an efficient catalytic system in water containing solution leaving room for optimization for instance by cobalt ligand exchange and/or different photosensitizers. A detailed study showed that by using 2,9-dimethyl-phenanthroline as a ligand for the cobalt complex a higher hydrogen yield with respect to the bipyridine ligand was achieved under nonaqueous conditions in DMF/triethanolamine (TEOA) 2:1. With **PS1** as the sensitizer the efficiency of H_2 formation under irradiation for 15 h using a 400 nm cut-off filter is determined by the nature of cobalt ligands; assuming complex formation *in situ*, as follows: 2,9-dimethylphenanthroline (dmphen) (**L1**) > 2,9-dimethyl-4,7-diphenyl-phenanthroline (dmdphphen) > disodium 2,9-dimethyl-4,7-diphenyl-phenanthroline-4′,4″-disulfonate > 4,4′-dimethyl-2,2′-bipyridine (dmbpy) > 3,3′-dimethyl-2,2′-bipyridine (dm′bpy) > 4,4′,5,5′-tetramethyl-2,2′-bipyridine (tmbpy) > 2,2′-bipyridine > phenanthroline (phen) > vitamin B_{12} > 4,7-diphenyl-phenanthroline [27]. Interestingly when **43** was irradiated with UV light ($\lambda > 300$ nm) with no ruthenium sensitizer present CO and H_2 were also produced. This observation suggests that excited state cobalt complexes may oxidize water [30] and/or the sacrificial electron donor [31] and that this process results in the formation of a reducing compound able to reduce CO_2 and H_2O to CO and H_2 [27].

A detailed investigation into the effect of different photosensitizers on the catalytic activity of these multicomponent systems has been performed using **44** as catalytic centre. In 50:50 water/acetonitrile solution with added 0.4 mL 12 M HCl containing 50 μM photosensitizer and 2.5 mM **44**, 0.57 M TEOA, 0.27 M LiCl turnover numbers reported for **44** sensitized with different ruthenium or iridium complexes are: $[Ru(bpy)_3]^{2+}$ (TON 2) (**PS1**) < $[Ru(dmphen)_3]^{2+}$ (**PS2**) (TON 12) < $[Ir(ppy)_2(bpy)]^+$ (**PS3**) (ppy = 2-phenylpyridine) (TON 16) < $[Ir(ppy)_2(phen)]^+$ (**PS4**) (TON 17) = $[Ir(ppy)_2(dphphen)]^+$ (**PS5**) = $[Ir(F\text{-}mppy)_2(phen)]^+$ (**PS6**) (F-mppy = 2-(4-fluorophenyl)-5-methylpyridine) = $[Ir(F\text{-}mppy)_2(dphphen)]^+$ (**PS7**) < $[Ir(F\text{-}mppy)_2(bpy)]^+$ (**PS8**) (TON 18) [32]. Further optimization of iridium based photosensitizers resulted in a $[Ir(dF(CF_3)ppy)_2(tbbpy)]^+$ ($dF(CF_3)ppy$ = 2-(2,4-difluorophenyl)-5-trifluoro-methylpyridine; tbbpy = 4,4′-di-*tert*-butyl-2,2′-bipyridine) (**PS9**, Fig. 6) complex which nearly double the hydrogen yield compared with $[Ru(dmphen)_3]^{2+}$ in a system of water containing acetonitrile/TEOA illuminated with 500 mW LEDs at 465 nm for 40 h under deoxygenated conditions [33].

The best yields are reported for the iridium based sensitizers having a longer excited state lifetime and a better quantum efficiency compared to ruthenium based sensitizers. When water is present the cobalt bipyridine complexes work more efficient than their phenanthroline derivatives. However, due to a broad variety of other reaction parameters the given trends are only true for the specified reaction conditions.

3.2. *Co glyoximes*

In 1979 the first investigations of the catalytic properties of cobaloximes as hydrogen evolving catalyst were undertaken by Oishi et al. These authors observed hydrogen evolution by visible light irradiation ($\lambda > 425$ nm) in an acetonitrile solution containing benzenethiolato-pyridine-bis-(dimethylglyoximato)cobalt(III) and benzenethiol [34]. The hydrogen yield was depending on the thioketone concentration in solution. The cobalt complex photocatalysed disulfide formation of benzenethiol effectively.

In the 1980s Hawecker et al. studied the properties of a photocatalytic system consisting of **PS1** and $Co(dmgH)_2$ ($dmgH_2$ = dimethylglyoxime), **23**, with a range of other solvent molecules as axial ligands [35]. This system, when irradiated with visible light ($\lambda > 400$ nm), in DMF with TEOA as a sacrificial electron donor and added $dmgH_2$ to stabilize the cobalt complex, gives a TON of 16 based on Co after 1 h. Addition of water led to a decrease of the hydrogen production rate. The stability of the catalytic constituents notably the photosensitizer seemed to be determining the

$$[Ru(bpy)_3]^{2+} + (h\nu) \rightarrow {}^*[Ru(bpy)_3]^{2+} \quad (3)$$

$$^*[Ru(bpy)_3]^{2+} + TEOA \rightarrow [Ru(bpy)_3]^{+} + TEOA^{+} \quad (4)$$

$$TEOA \rightarrow \text{decomposition products} \quad (5)$$

$$[Ru(bpy)_3]^{+} + Co(II)dmgH_2 \leftrightarrow [Ru(bpy)_3]^{2+} + [Co(I)dmgH_2]^{-} \quad (6)$$

$$[Co(I)dmgH_2]^{-} + H^{+} + S \leftrightarrow HCo(III)(dmgH)_2(S) \quad (7)$$

$$HCo(III)(dmgH)_2(S) + H_3O^{+} \rightarrow [(H_2O)Co(III)(dmgH)_2(S)]^{+} + H_2 \quad (8)$$

$$2\ HCo(III)(dmgH)_2(S) \rightarrow 2\ Co(II)(dmgH)_2 + H_2 + S \quad (9)$$

$$[(H_2O)Co(III)(dmgH)_2(S)]^{+} + e^{-} \rightarrow Co(II)(dmgH)_2 + H_2O + S \quad (10)$$

$$[(H_2O)Co(III)(dmgH)_2(S)]^{+} + HCo(III)(dmgH)_2(S) \rightarrow 2\ Co(II)(dmgH)_2 + H_3O^{+} + 2S \quad (11)$$

Scheme 1. Reactions leading to H_2 in the photocatalytic process with ruthenium photosensitizers.

efficiency. Experiments carried out over an 18 h period show that hydrogen evolution slowed down within 9 h increasing again to a nearly initial H_2 production rate when further **PS1** was added. Evidence for the degradation of the cobalt complex during the catalysis was obtained by addition of $P(n\text{-}Bu)_3$ to the solution. An increased TON of 88 for the *in situ* produced phosphine stabilized cobalt complex after 6.5 h irradiation is reported suggesting that the phosphine might stabilize the intermediate cobalt(I) species. The catalytic performance is also dependent on the pH of the solution used. An optimal performance was found within a pH range between 8.6 and 8.9 in DMF/TEOA or $CH_3CN/TEOA/H_2O$, respectively. A reasonable mechanism involves Co(III) hydride species as discussed before in Section 2.1 (Eqs. (1) and (2)) and as shown in Eqs. (3)–(11) (Scheme 1). The proposed catalytic cycle by Lehn et al. is shown in Fig. 7.

Eqs. (8) and (9) show that starting from a Co(III) hydride species two different reactions lead to the formation of hydrogen. A protonation of the hydride would result in hydrogen formation and Co(III) complex generation (8). The other alternative would be a reaction of two Co(III)-hydride complexes under liberation of hydrogen and generation of the Co(II) complexes (9). The later seems to be more likely based on the results of electrocatalytic hydrogen production in Section 2.1 [12,13]. Regeneration from Co(III) to the initial Co(II) complex is given in (10) and (11).

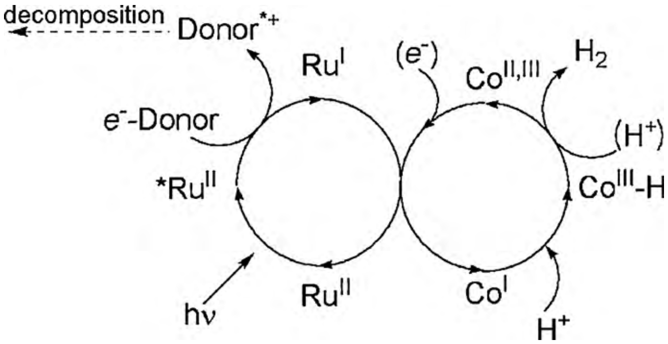

Fig. 7. Photocatalytic cycle as proposed by Lehn et al. [35].

$[Re(CO)_3Br(phen)]$ (**PS10**) has been investigated as photosensitizer by Artero et al., Fig. 8 [36]. Under irradiation with visible light (15 h) ($\lambda > 380$ nm) a TON of 273 was obtained in acetone, 600 equiv. of Et_3N and Et_3NH^+ in the presence of **PS10** and **26** as catalytic centre. It is important to note here that Re(I)-carbonyl complexes are seemingly involved in hydrogen evolution themselves [37]. Hamm et al. studied the hydrogen production process using a bipyridine rhenium complex as a photosensitizer (**PS11**, Fig. 8) and $Co(dmgH)_2$ as a catalyst [38]. In an oxygen free DMF solution with AcOH as the proton source and the electron donor TEOA, **PS11**, $Co(OAc)_2{\cdot}4H_2O$ and a sixfold excess of $dmgH_2$ a TON of 75 with respect to the cobalt centre (TON 150 defined as H_2 per photosensitizer) was achieved after 9 h irradiation ($\lambda \geq 400$ nm).

Eisenberg et al. have investigated Pt(II) terpyridine phenylacetylide complexes such as **PS12** and **PS13** (Fig. 9) in combination

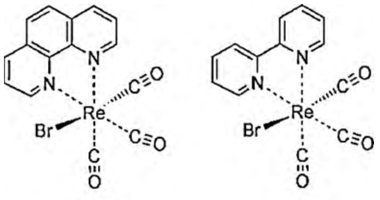

PS10 PS11

Fig. 8. Rhenium based photosensitizers.

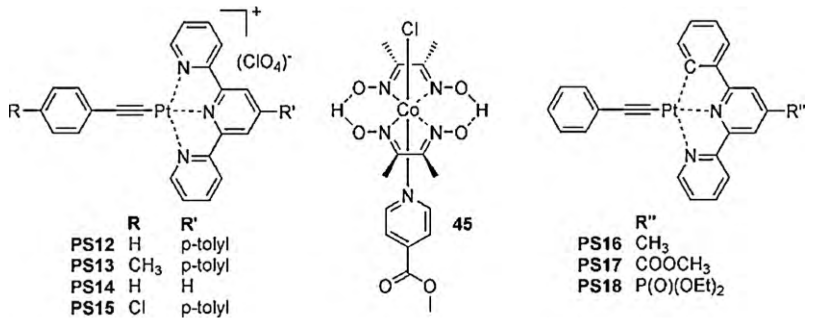

Fig. 9. Photosensitizers used by Eisenberg et al. and a modified cobaloxime complex.

with various cobaloxime complexes [39–41]. The reaction mixture containing **17**, **PS12** and TEOA in CH_3CN/H_2O (3:2 v/v) at pH 8.5 irradiated with visible light ($\lambda > 410$ nm) produced hydrogen with a TON after 10 h of ~23 based on the cobalt catalyst (TON ~400 based on Pt). Increasing the TEOA concentration to 0.27 M the TON increases to ~56 with respect to cobalt after 10 h (TON ~1000 based on Pt). Optimized reaction conditions, of a CH_3CN/H_2O mixture (24:1 v/v) and 0.27 M TEOA as sacrificial electron donor leads to a roughly twofold increase in TON (TON ~119 with respect to cobalt, ~2150 based on **PS12**) after 10 h [41]. When altering the pH to more acidic or basic conditions hydrogen production decreases dramatically. The combination of **PS12** and **26** (axial ligands can be different) under the same conditions did not lead to hydrogen production upon irradiation. This observation shows that not all general trends gathered from electrocatalytic reactions can be applied directly to photocatalysis. No hydrogen formation was observed when **PS12** was substituted by **PS1** in combination with **17**. The catalytic activity in these investigations strongly correlates with the properties of the photocentres. The reaction rates follow the order **PS13** > **PS14** > **PS15** > **PS12**. As one of the most effective system under the reaction conditions mentioned above **PS13** in combination with **30** (Fig. 9) is noted, but the hydrogen yield is not defined. Hydrogen production activity of the cyclometalated photosensitizer **PS16** with **17** is reported with a TON of 170 (94 based on Co) in 5 h, **PS17** and **PS18** give a TON of 90 (50 based on Co) and 120 (66 based on Co) within 5 h, respectively.

A recently presented noble metal free approach with eosins as a photosensitizer produces hydrogen in aqueous solution [42]. The reaction mixture consists of a CH_3CN/H_2O solution (1:1) at pH 7, 5% (v) TEOA, eosin Y (**PS19**, Fig. 10) and **17** with a 12-fold excess of free $dmgH_2$ giving a TON of 181 *vs.* **17** (~900 *vs.* **PS19**) after 12 h illumination, $\lambda > 450$ nm. Hydrogen evolution stops while the solution bleaches due to degradation of the dye and the cobalt complex. The degradation can be slowed by adding excess of $dmgH_2$ to the system resulting in stabilization of both, dye and cobalt catalyst. Irradiation with light $\lambda = 520$ nm, which corresponds to the absorption maximum of **PS19**, over 24 h and under similar reaction conditions yielded a TON of ~40 *vs.* Co (~200 *vs.* **PS19**) with a constant rate for hydrogen production due to markedly better photostability.

3.3. Cobalt cyclam, porphyrin and corrin complexes

In the late 1970s Endicott et al. reported the homogenous catalysis of the photoreduction of water by visible light [43]. They used the photosensitizer **PS1**, a cobalt(II) cyclam macrocycle, $Me_6[14]dieneN_4\text{-}(H_2O)_2^{2+}$ (**1**H_2O) and ascorbate or Eu(II) ions as electron donor in aqueous solution yielding hydrogen at irradiation with visible light (λ 450 nm ± 20 nm) with an overall quantum yield of 0.05. Broad-band irradiation with a 405 nm long-pass filter gave a TON value of ~1. The hydrogen production decreases with increasing photolysis times. Yanagida and co-workers investigated various cobalt cyclam derivatives in combination with a p-terphenyl sensitizer (**PS20**, Fig. 11) where **46** (Fig. 11) gave the best results for hydrogen production in a water containing TEA/acetonitrile/water mixture (1:4:1) under argon [44]. The combination **PS20** with **46** generates hydrogen as the only product with a TON of 17 after 1 h (calculated from experimental details) by irradiation with light $\lambda > 290$ nm.

Yanagida et al. have reported that upon UV-irradiation of phenazine photosensitizer (**PS21**, Fig. 11), **46** and TEA as the electron donor in methanolic solution under a CO_2 atmosphere, apart from formate hydrogen is produced as a secondary product. Hydrogen evolution was also observed in the absence of CO_2. The sensitization process is thought to occur via a phenazine radical anion formed by the reaction of the excited phenazine molecule in its triplet state with TEA and is able to reduce Co(III) to Co(II) [45].

Neta et al. studied the reaction of **PS20** with a cobalt porphyrin complex **47** in CO_2 saturated acetonitrile, containing 5% TEA, where upon irradiation with light $\lambda > 300$ nm H_2 was evolved as a side reaction in competition with CO_2 reduction [46]. Investigations with vitamin B_{12} derivatives (Fig. 12) in combination with **PS20** showed H_2 as a product in a solution of acetonitrile/methanol (9:1 v:v), 5% TEA, saturated with CO_2, interestingly in higher yields compared to CO for the CO_2 reduction reaction [47]. In the presence of He instead of CO_2 cyanocobalamin (**48**) showed the highest hydrogen yield compared to hydroxocobalamin (**49**) > cobinamide (**50**) > hydroxocobalamin > **47**.

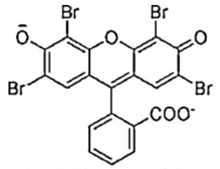

Eosin Y **PS19**

Fig. 10. Eosin used as photosensitizer in the hydrogen evolution reaction with cobaloximes.

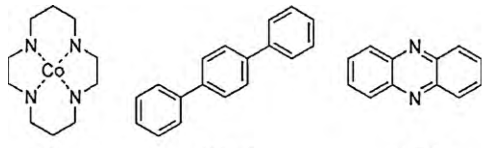

46 **PS20** **PS21**

Fig. 11. Cobalt cyclam complex, counter ions, charges and axial ligands omitted (**27**), and organic photosensitizers p-terphenyl (**PS20**) and phenazine (**PS21**).

Table 2

Selected combinations of cobalt complexes and photosensitizers or intramolecular assemblies for photocatalytic hydrogen production.

No. Co complex	No. photosensitizer	λ irradiation	Sacrificial electron donor	Solvent system	Product	TON *vs.* Co	Ref.
28	**PS1**	>400 nm	n-Pr_3N	$CH_3CN/H_2O/n\text{-}Pr_3N$ (3:1:1); CO_2	CO + H_2	9 (22 h)	[25]
28	**PS1**	>400 nm	Et_3N	$CH_3CN/H_2O/Et_3N$, CO_2, 10 equiv. bpy *vs.* Co	CO decreased, H_2 increased *vs.* line 1	[a]	[25]
28	–	>300 nm	TEOA	CH_3CN or DMF, TEOA, H_2O, CO_2	CO + H_2	[a]	[27]
$CoL1_3{}^{2+}$	**PS1**	>400 nm	TEOA	DMF/TEOA (2:1)	CO + H_2	26 (15 h)	[27]
29	**PS1**	465 nm	TEOA	CH_3CN/H_2O (1:1), TEOA, LiCl, HCl	H_2	2	[32]
29	**PS2**	465 nm	TEOA	CH_3CN/H_2O (1:1), TEOA, LiCl, HCl	H_2	12	[32]
29	**PS3**	465 nm	TEOA	CH_3CN/H_2O (1:1), TEOA, LiCl, HCl	H_2	16	[32]
29	**PS4**	465 nm	TEOA	CH_3CN/H_2O (1:1), TEOA, LiCl, HCl	H_2	17	[32]
29	**PS5**	465 nm	TEOA	CH_3CN/H_2O (1:1), TEOA, LiCl, HCl	H_2	17	[32]
29	**PS6**	465 nm	TEOA	CH_3CN/H_2O (1:1), TEOA, LiCl, HCl	H_2	17	[32]
29	**PS7**	465 nm	TEOA	CH_3CN/H_2O (1:1), TEOA, LiCl, HCl	H_2	17	[32]
29	**PS8**	465 nm	TEOA	CH_3CN/H_2O (1:1), TEOA, LiCl, HCl	H_2	18	[32]
29	**PS9**	465 nm	TEOA	CH_3CN/H_2O (1:1), TEOA, LiCl, HCl	H_2	[a]	[33]
19[b]	**PS1**	>400 nm	TEOA	DMF, TEOA, $dmgH_2$	H_2	16 (1 h)	[35]
19[b]	**PS1**	>400 nm	TEOA	DMF, TEOA, $dmgH_2$, $P(n\text{-}Bu)_3$	H_2	88 (6.5 h)	[35]
22	**PS10**	>380 nm	Et_3N	Acetone, Et_3N, Et_3NHBF_4	H_2	273 (15 h)	[36]
19[b]	**PS11**	≥400 nm	TEOA	DMF, AcOH, TEOA, $dmgH_2$	H_2	75 (9 h)	[38]
13	**PS12**	>410 nm	TEOA	CH_3CN/H_2O (3:2), $c_{TEOA} = 1.61 \times 10^{-2}$ M, pH 8.5	H_2	23 (10 h)	[40]
13	**PS13**	>410 nm	TEOA	CH_3CN/H_2O (3:2), $c_{TEOA} = 0.27$ M, pH 8.5	H_2	56 (10 h)	[40]
13	**PS14**	>410 nm	TEOA	CH_3CN/H_2O (24:1), $c_{TEOA} = 0.27$ M, pH 8.5	H_2	119 (10 h)	[41]
13	**PS12**, **PS16**	>410 nm	TEOA	CH_3CN/H_2O (24:1), $c_{TEOA} = 1.61 \times 10^{-2}$ M, pH 8.5	H_2	94 (5 h)	[41]
13	**PS17**	>410 nm	TEOA	CH_3CN/H_2O (24:1), $c_{TEOA} = 1.61 \times 10^{-2}$ M, pH 8.5	H_2	50 (5 h)	[41]
13	**PS18**	>410 nm	TEOA	CH_3CN/H_2O (24:1), $c_{TEOA} = 1.61 \times 10^{-2}$ M, pH 8.5	H_2	66 (5 h)	[41]
13	**PS19**	>450 nm	TEOA	CH_3CN/H_2O (1:1), TEOA (5%), $dmgH_2$, pH 7	H_2	181 (12 h)	[42]
13	**PS19**	>520 nm	TEOA	CH_3CN/H_2O (1:1), TEOA (5%), $dmgH_2$, pH 7	H_2	40 (24 h)	[42]
PS-Co1		>350 nm	Et_3N	Acetone, Et_3N, Et_3NH	H_2	103 (15 h)	[53]
PS-Co2		>380 nm	Et_3N	Acetone, Et_3N, Et_3NH	H_2	9 (4 h)	[36]
PS-Co3		>380 nm	Et_3N	Acetone, Et_3N, Et_3NH	H_2	210 (15 h)	[36]
PS-Co4[c]		470 nm	Et_3N	MeOH, c(H_2O) 2.78 M, Et_3N, $dmgH_2$	H_2	235 (20 h)	[55]
PS-Co5[c]		470 nm	Et_3N	MeOH, c(H_2O) 5.55 M, Et_3N, $dmgH_2$	H_2	58 (24 h)	[55]
PS-Co6[c]		470 nm	Et_3N	MeOH, c(H_2O) 5.55 M, Et_3N, $dmgH_2$	H_2	32 (24 h)	[55]
PS-Co7[c]		470 nm	Et_3N	MeOH, c(H_2O) 5.55 M, Et_3N, $dmgH_2$	H_2	2 (24 h)	[55]
PS-Co8		>400 nm	Et_3N	Acetone, Et_3N, [Et3NH][BF_4]	H_2	38 (8 h)	[56]
PS-Co9		>400 nm	Et_3N	Acetone, Et_3N, [Et_3NH][BF_4]	H_2	48 (8 h)	[56]

[a] Not defined.

[b] Solvent dependent axial ligand exchange possible.

[c] Under aerobic conditions.

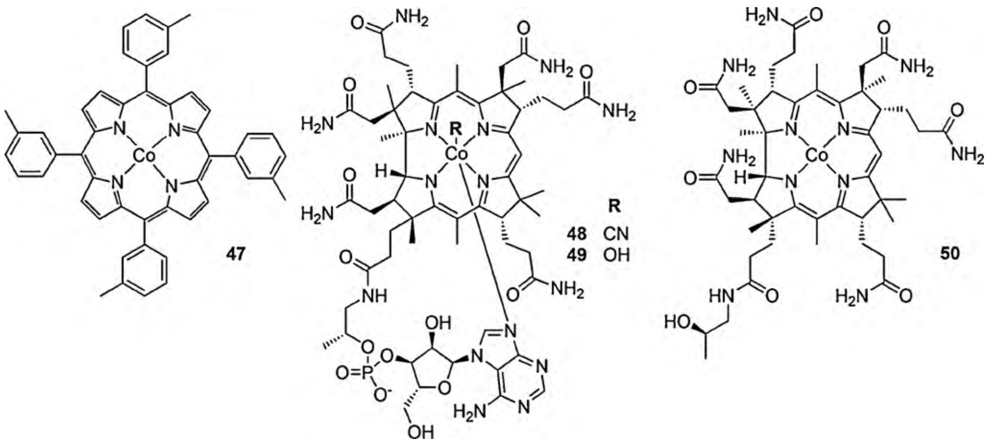

Fig. 12. Cobalt porphyrin and corrin complexes; CoTTP, cyanocobalamin, hydroxocobalamin and cobinamide (axial ligands omitted).

3.4. Polypyridine, cyclopentadienyl and inorganic cobalt complexes

Cobalt complexes of polypyridine ligands like ttp (**51**) or pdt (**52**) were studied by Königstein and Bauer [48]. They reported that in aqueous solution these cobalt complexes can produce hydrogen in the presence of the photosensitizer **PS1** and ascorbic acid as electron donor. Complex **52** is more efficient than **51** and showed during the initial phase of catalysis high reaction rates with quantum yields for H_2 formation in the range of 20%, but the complex decomposes during the reaction resulting in lower quantum yield for the overall process (~1%). Ligand loss is discussed as one of the main problems during the reaction. Complex **51** does not show ligand loss but the activity is lower with quantum yields <1% (Fig. 13).

Kölle et al. presented hydrogen producing cobalt cyclopentadienyl derivatives. Using pulse radiolysis methods in Ar degassed aqueous solutions of sulfuric acid in 2-propanol under short irradiation times with $\lambda > 320$ nm indicates that **53** is a suitable catalyst for hydrogen evolution [49]. Electrochemical and photochemical investigations as well as excited state quenching of **PS1** by **40** underline the suitability of $[Co(C_5H_4COOH)_2]$ as hydrogen generating relay [22]. Moreover different derivatives of cobalt sepulchrate cage complexes are discussed in the literature as possible catalysts for the photoreduction of water [22,24,50].

Research in the field of the photochemical behavior of cobalt cyanide complexes and their role in hydrogen evolution reactions was performed by Rozenkevich and co-workers [51,52]. They investigated hydrogen production by irradiation of $[Co(CN)_5H_2O]^{3-}$ in aqueous alcoholic solutions with light $\lambda > 320$ nm. The influence of CN ligand exchange with ammonia, ethylenediamine and monoethanolamine was investigated. Organic dyes like rhodamine-B, rhodamine-G and eosin (**PS19**) as well as **PS1** were used. When using dyes in a concentration window of $4–10 \times 10^{-5}$ mol L^{-1} hydrogen evolution rates did not change. Further increased concentrations led to a decreasing hydrogen production. Salt-additives such as MeCl (Me = Li^+, Na^+, K^+, Cs^+) increase hydrogen production especially in the case of LiCl [51,52].

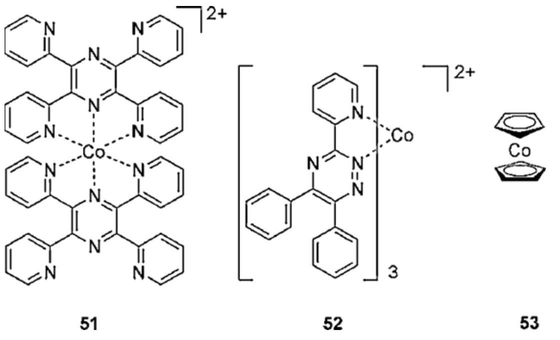

Fig. 13. Co complexes with ttp, pdt and cp ligands.

3.5. Supramolecular systems

A ruthenium bipyridine complex with a (4-pyridine)oxazolo-[4,5-f]phenanthroline ligand (**PS-Co1**, Fig. 14) where the pyridine ring can coordinate as an axial “ligand” for a cobaloxime type complex related to **26** has been investigated [53].

The reported maximum TON for the cobalt moiety is 103 after 15 h irradiation of a system containing the intramolecular system **PS-Co1** in acetone and Et_3N as the sacrificial electron donor, a 350 nm cut-off filter was used [36]. These detailed studies on the system indicated that the near UV range (315–380 nm) is responsible for the catalytic activity. The molecular catalyst **PS-Co1** showed no activity under irradiation with light $\lambda > 380$ nm. Substitution of the bipyridine ligands with phenanthrolines (**PS-Co2**, Fig. 14) led to lower hydrogen production (TON 9 after 4 h). However, when ruthenium is substituted by an iridium centre (**PS-Co3**, Fig. 14) hydrogen evolution increases dramatically. A TON of 210 was obtained after 15 h irradiation with visible light ($\lambda > 380$ nm) with **PS-Co3** in acetone, in the presence of 600 equiv. of Et_3N and Et_3NH^+.

In our group a photocatalytic assembly consisting of a ruthenium complex with a 4,4′-dicyano-2,2′-bipyridine ligand as photosensitizer (Scheme 2) has been studied [54]. The nitrile group was introduced to allow for the formation of a coordination bond between the Ru and Co centre **15**. UV/vis and emission data of the photocatalytic reaction involving both components show a significant change of the electronic properties of the ruthenium complex within the first 2 h of irradiation.

Mass spectrometry indicates amide formation as indicated by the successive addition of two 18 *m*/*z* fragments to the molecular ion during that same period. In addition, electrochemical investigations indicate the *in situ* formation of a ligand with a higher energy π^* orbital. The difference in emission wavelength between the dark reaction (emission at 665 nm) and the photoreaction (emission at 638 nm) shows that not only a base induced hydrolysis of the nitrile groups is responsible for this change. Detailed investigations to explain this finding are in progress. The structure of a possible molecular photocatalyst, **PS-Co4**, is shown in Fig. 15 [55]. Most importantly this system shows the best performance under aerobic conditions. Under optimized aerobic conditions (methanol/water mixture ($c(H_2O)$ 2.78 mol L^{-1}), Et_3N and a 40-fold excess of $dmgH_2$) a TON of 235 is obtained with respect to the cobalt centre after

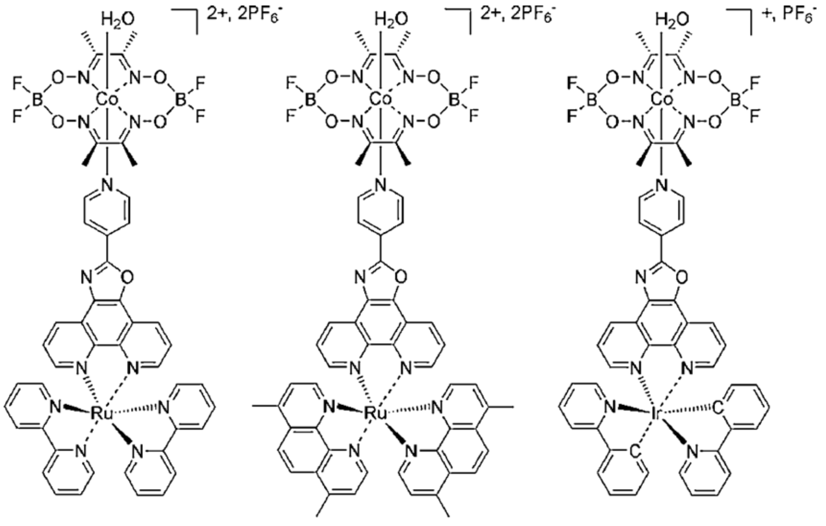

PS-Co1 **PS-Co2** **PS-Co3**

Fig. 14. Intramolecular photocatalysts based on ruthenium and iridium sensitizer subunits by Artero et al. [36,52].

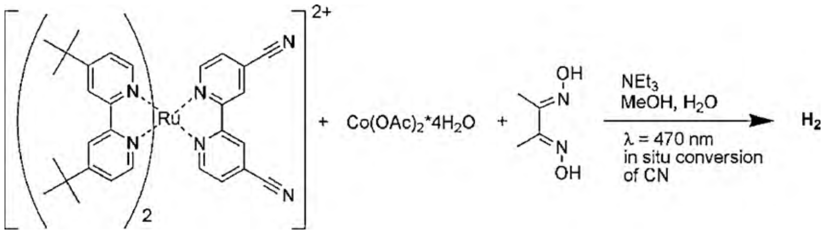

Scheme 2. Catalytic system for hydrogen evolution under aerobic conditions.

20 h of LED irradiation with λ = 470 nm. Under anaerobic conditions but otherwise similar reaction conditions the TON observed was 8 after 42 h. This is in total contrast to all other systems discussed in this review and this observation may play a significant role in the development of homogenous overall water splitting systems where oxygen will be the product of the water oxidation reaction. Ruthenium complexes with carboxylic acid groups, also able to interact with cobalt centres, showed lower hydrogen yields under similar reaction conditions with a water concentration of 5.55 mol L^{-1}. The activity is in the order [(bpy)$_2$Ru(4-Me,4′-COOH-2,2′-bipyridine)]$^{2+}$ (**PS-Co5**) (TON 58) > [(bpy)$_2$Ru(dcbpy)]$^{2+}$ (**PS-Co6**) (TON 32) > [(dcbpy)$_3$Ru]$^{2+}$ (**PS-Co7**) (TON 2) after a 24 h irradiation, λ = 470 nm.

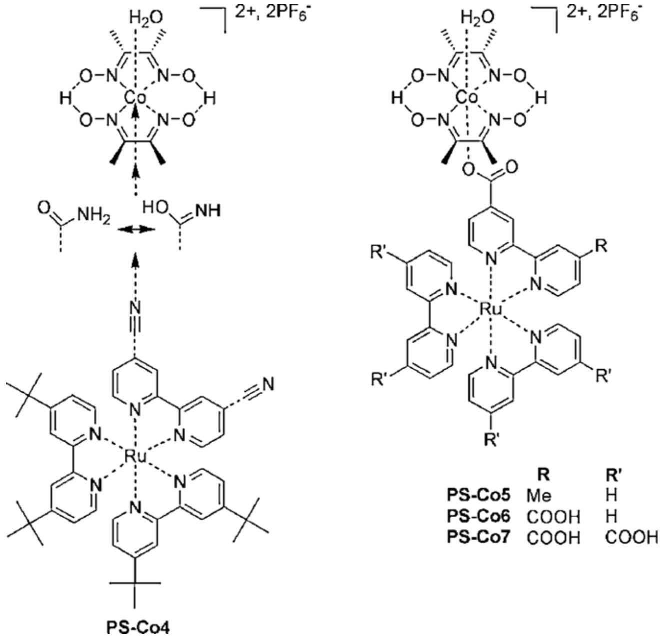

	R	R′
PS-Co5	Me	H
PS-Co6	COOH	H
PS-Co7	COOH	COOH

PS-Co4

Fig. 15. Intramolecular photocatalytic systems for photocatalytic hydrogen production with possible interaction.

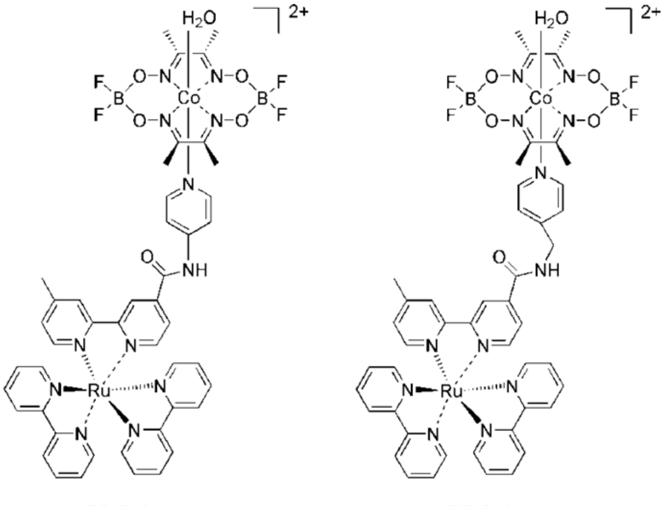

PS-Co8 **PS-Co9**

Fig. 16. Intramolecular photocatalysts for hydrogen production with visible light by Sun et al. [56].

Sun and co-workers have presented two photocatalysts connecting the ruthenium centre with the cobalt moiety via a pyridine which is bound to a bipyridine unit over an amide function (Fig. 16) [56]. In **PS-Co8** the pyridine is in conjugation with the amide, in **PS-Co9** an inserted methylene group leads to an unconjugated bonding. In acetone and Et_3N as the sacrificial electron donor **PS-Co8** gives a TON of 38 after 8 h by irradiation with light $\lambda > 400$ nm and $[Et_3NH][BF_4]$ as the proton source. Interestingly with **PS-Co9** a TON of 48 has achieved under the same conditions which is discussed by depressing the electron transfer back reaction using an unconjugated pyridine unit (Table 2).

4. Conclusion and outlook

The electrocatalytic hydrogen formation highlights the importance of this method for the optimization of cobalt complexes capable of catalysing hydrogen evolution. Of particular importance is the potential at which the electrocatalysts become active. For example, it has been shown that cobalt cyclam macrocycles are able to electrocatalyse the hydrogen evolution process but cobalt porphyrins have a more positive reduction potential, able to form hydrogen at ~ -0.95 V *vs.* SCE. The large group of cobalt glyoxime complexes, with the possibility of axial ligand exchange, shows also good catalytic activity when potentials ~ 0.95 V *vs.* SCE are applied. The introduction of boron (BF_2) containing bridges in the ligand framework results in increased catalytic activity most likely induced by increased rigidity of the macrocyclic ligand complexes in this range and sepulchrate complexes of cobalt are active at even -0.7 V *vs.* SCE. It is important to note that hydrogen production occurs in nearly all cases at a ~ -0.9 to -1.0 V *vs.* SCE. This suggests that photosensitizers applied in photocatalytic studies should be able to reduce the cobalt centres within this potential window. An interesting angle is the incorporation of cobalt phthalocyanines in a poly(4-vinylpyridine-co-styrene) film this such a modified electrode shows very high turnover frequencies. This underlines the importance of the stabilization of the catalytically active metal centre, which has been accomplished here by interaction with the polymer side chain pyridine functions. These results are very important for the correct choice of catalytic centres also in photocatalytic applications.

Redox active complexes based on rhenium, ruthenium, iridium or platinum as well as organic dyes have been used for the photosensitization of cobalt complexes to produce hydrogen. The complexity of the homogenous catalytic mixture consisting of the solvent, sometimes water or anhydrous proton sources, sacrificial electron donors, different types of photosensitizers and catalytic active cobalt centres, additives and different atmospheres of CO_2, argon or N_2 makes it difficult to compare and contrast the published studies. In addition the use of different wavelength and light intensities for irradiation further complicates the issue. But turnover values can be used for indirect comparison. Considering the TONs with respect to the cobalt centre the top four of the most active photosensitizer/cobalt complex combination is (I) the rhenium based photosensitizer **PS10** and **26** (II) the ruthenium complex **PS-Co4** and Co glyoxime moiety (III) the iridium based supramolecular assembly **PS-Co3** and (IV) **PS19** with **17** (an eosin dye and a cobalt glyoxime complex with a chloride and pyridine as the axial ligands).

This review shows that there is considerable potential for new promising combinations or optimization. Significant problems need however to be overcome. The main one being the general use of sacrificial agents in photocatalytic systems. Their need will cancel any environmental benefits the photocatalytic route may have. The electrocatalytic approach has a clear advantage in this respect. Another concern is also the general use with one exception of oxygen free solvents. Oxygen is inevitably formed in the process of water splitting and therefore systems like **PS-Co4** working under an oxygen containing atmosphere can be the first step to future homogenous overall water splitting systems.

Acknowledgments

S.L. wants to thank the DBU (German Federal Environmental Foundation) for financial support. Science Foundation Ireland has contributed to this research with Grant No. 07/SRC/B1160 Advanced Biomimetic Materials for Solar Energy Conversion (JGV). S.R. acknowledges financial support from the Deutsche Forschungs Gemeinschaft (GRK 1626, SFB 583).

References

[1] N. Armaroli, V. Balzani, Angew. Chem. Int. Ed. 46 (2007) 52.

[2] D. Walther, M. Ruben, S. Rau, Coord. Chem. Rev. 182 (1999) 67.

[3] M.W. Kanan, D.G. Nocera, Science 321 (2008) 1072.

[4] J. Rosenthal, J. Bachman, J.L. Dempsey, A.J. Esswein, T.G. Gray, J.M. Hodgkiss, D.R. Manke, T.D. Luckett, B.J. Pistorio, A.S. Veige, D.G. Nocera, Coord. Chem. Rev. 249 (2005) 1316.

[5] M.W. Kanan, Y. Surendranath, D.G. Nocera, Chem. Soc. Rev. 38 (2008) 109.

[6] T.J. Meyer, Nature 451 (2008) 778.

[7] B.J. Fisher, R. Eisenberg, J. Am. Chem. Soc. 102 (1980) 7361.

[8] J.P. Bigi, T.E. Hanna, W.H. Harman, A. Chang, C.J. Chang, Chem. Commun. 46 (2010) 958.

[9] N.K. Szymczak, L.A. Berben, J.C. Peters, Chem. Commun. (2009) 6729.

[10] R.M. Kellett, T.G. Spiro, Inorg. Chem. 24 (1985) 2373.

[11] R.M. Kellett, T.G. Spiro, Inorg. Chem. 24 (1985) 2378.

[12] J.L. Dempsey, B.S. Brunschwig, J.R. Winkler, H.B. Gray, Acc. Chem. Res. 42 (2009) 1995.

[13] J.L. Dempsey, J.R. Winkler, H.B. Gray, J. Am. Chem. Soc. 132 (2010) 1060.

[14] F. Zhao, J. Zhang, T. Abe, D. Wöhrle, M. Kaneko, J. Mol. Catal. A: Chem. 145 (1999) 245.

[15] M. Razavet, V. Artero, M. Fontecave, Inorg. Chem. 44 (2005) 4786.

[16] X. Hu, B.M. Cossairt, B.S. Brunschwig, N.S. Lewis, J.C. Peters, Chem. Commun. (2005) 4723.

[17] X. Hu, B.S. Brunschwig, J.C. Peters, J. Am. Chem. Soc. 129 (2007) 8988.

[18] C. Baffert, V. Artero, M. Fontecave, Inorg. Chem. 46 (2007) 1817.

[19] P.-A. Jacques, V. Artero, J. Pécaut, M. Fontecave, Proc. Natl. Acad. Sci. 106 (2009) 20627.

[20] L.A. Berben, J.C. Peters, Chem. Commun. 46 (2010) 398.

[21] U. Koelle, S. Ohst, Inorg. Chem. 25 (1986) 2689.

[22] V. Houlding, T. Geiger, U. Kölle, M. Grätzel, J. Chem. Soc., Chem. Commun. (1982) 681.

[23] G.M. Jacobsen, J.Y. Yang, B. Twamley, A.D. Wilson, R.M. Bullock, M.R. DuBois, D.L. DuBois, Energy Environ. Sci. 1 (2008) 167.

[24] P.A. Lay, A. Mau, W.H.F. Sasse, I.I. Creaser, L.R. Gahan, A.M. Sargeson, Inorg. Chem. 22 (1983) 2347.

[25] J.-M. Lehn, R. Ziessel, Proc. Natl. Acad. Sci. U.S.A. 79 (1982) 701.

[26] M. Kirch, J.-M. Lehn, J.-P. Sauvage, Helv. Chim. Acta 62 (1979) 1345.

[27] R. Ziessel, J. Hawecker, J.M. Lehn, Helv. Chim. Acta 69 (1986) 1065.

[28] C.V. Krishnan, N. Sutin, J. Am. Chem. Soc. 103 (1981) 2141.

[29] C.V. Krishnan, B.S. Brunschwig, C. Creutz, N. Sutin, J. Am. Chem. Soc. 107 (1985) 2005.

[30] D.R. Eaton, S.R. Suart, J. Phys. Chem. 72 (1968) 400.

[31] M. Wolfsberg, L. Helmholz, J. Chem. Phys. 20 (1952) 837.

[32] J.I. Goldsmith, W.R. Hudson, M.S. Lowry, T.H. Anderson, S. Bernhard, J. Am. Chem. Soc. 127 (2005) 7502.

[33] M.S. Lowry, J.I. Goldsmith, J.D. Slinker, R. Rohl, R.A. Pascal, G.G. Malliaras, S. Bernhard, Chem. Mater. 17 (2005) 5712.

[34] S. Oishi, K. Nozaki, Chem. Lett. (1979) 549.

[35] J. Hawecker, J.M. Lehn, R. Ziessel, J. New. Chem. Nouveau J. Chim. 7 (1983) 271.

[36] A. Fihri, V. Artero, A. Pereira, M. Fontecave, Dalton Trans. (2008) 5567.

[37] B. Gholamkhass, H. Mametsuka, K. Koike, T. Tanabe, M. Furue, O. Ishitani, Inorg. Chem. 44 (2005) 2326.

[38] B. Probst, C. Kolano, P. Hamm, R. Alberto, Inorg. Chem. 48 (2009) 1836.

[39] P. Du, J. Schneider, P. Jarosz, J. Zhang, W.W. Brennessel, R. Eisenberg, J. Phys. Chem. B 111 (2007) 6887.

[40] P. Du, K. Knowles, R. Eisenberg, J. Am. Chem. Soc. 130 (2008) 12576.

[41] P. Du, J. Schneider, G. Luo, W.W. Brennessel, R. Eisenberg, Inorg. Chem. 48 (2009) 4952.

[42] T. Lazarides, T. McCormick, P. Du, G. Luo, B. Lindley, R. Eisenberg, J. Am. Chem. Soc. 131 (2009) 9192.

[43] G.M. Brown, B.S. Brunschwig, C. Creutz, J.F. Endicott, N. Sutin, J. Am. Chem. Soc. 101 (1979) 1298.

[44] S. Matsuoka, K. Yamamoto, T. Ogata, M. Kusaba, N. Nakashima, E. Fujita, S. Yanagida, J. Am. Chem. Soc. 115 (1993) 601.

[45] T. Ogata, Y. Yamamoto, Y. Wada, K. Murakoshi, M. Kusaba, N. Nakashima, A. Ishida, S. Takamuku, S. Yanagida, J. Phys. Chem. 99 (1995) 11916.

[46] T. Dhanasekaran, J. Grodkowski, P. Neta, P. Hambright, E. Fujita, J. Phys. Chem. A 103 (1999) 7742.

[47] J. Grodkowski, P. Neta, J. Phys. Chem. A 104 (2000) 1848.

[48] C. Königstein, R. Bauer, Int. J. Hydrogen Energy 22 (1997) 471.
[49] U. Koelle, P.P. Infelta, M. Graetzel, Inorg. Chem. 27 (1988) 879.
[50] I.I. Creaser, R.J. Geue, J.M. Harrowfield, A.J. Herlt, A.M. Sargeson, M.R. Snow, J. Springborg, J. Am. Chem. Soc. 104 (1982) 6016.
[51] M.B. Rozenkevich, J.A. Sakharovsky, Int. J. Hydrogen Energy 14 (1989) 431.
[52] E. Smirnova, V. Ermakov, M. Rozenkevich, Kinet. Catal. 41 (2000) 48.
[53] A. Fihri, V. Artero, M. Razavet, C. Baffert, W. Leibl, M. Fontecave, Angew. Chem. Int. Ed. 47 (2008) 564.
[54] S. Losse, H. Görls, R. Groarke, J.G. Vos, S. Rau, Eur. J. Inorg. Chem. (2008) 4448.
[55] S. Losse, R. Groarke, J.G. Vos, I. Ivanovic-Burmazovic, S. Rau, in preparation.
[56] C. Li, M. Wang, J. Pan, P. Zhang, R. Zhang, L. Sun, J. Organomet. Chem. 694 (2009) 2814.